Archives of Biochemistry and Biophysics 480 (2008) 95–103

Contents lists available at ScienceDirect

Archives of Biochemistry and Biophysics

journal homepage: www.elsevier.com/locate/yabbi

A novel activating effect of the regulatory subunit of protein kinase A on catalytic subunit activity

Jimena Rinaldi, Josefina Ocampo, Silvia Rossi, Silvia Moreno *

Departamento de Química Biológica, Facultad de Ciencias Exactas y Naturales, Universidad de Buenos Aires, Ciudad Universitaria, Pabellón 2, Piso 4, 1428 Buenos Aires, Argentina

ARTICLE INFO

Article history:
Received 10 July 2008
and in revised form 23 September 2008
Available online 30 September 2008

Keywords:
Protein kinase A
Peptides
Linker domain I
Substrates
Regulatory subunit
Inhibition
Activation

ABSTRACT

The strength of the interaction between the catalytic and regulatory subunits in protein kinase A differs among species. The linker region from regulatory subunits is non-conserved. To evaluate the participation of this region in the interaction with the catalytic subunit, we have assayed its effect on the enzymatic properties of the catalytic subunit. Protein kinase A from three fungi, *Mucor rouxii*, *Mucor circinelloides* and *Saccharomyces cerevisiae* have been chosen as models. The R–C interaction is explored by using synthetic peptides of 8, 18 and 47 amino acids, corresponding to the R subunit autophosphorylation site plus a variable region toward the N terminus (0, 10, or 39 residues). The K_m of the catalytic subunits decreased with the length of the peptide, while the V_{max} increased. Viscosity studies identified product release as the rate limiting step for phosphorylation of the longer peptides. Pseudosubstrate derivatives of the 18 residue peptides did not display a competitive inhibition behavior toward either kemptide or a *bona fide* protein substrate since, at low relative pseudosubstrate/substrate concentration, stimulation of kemptide or protein substrate phosphorylation was observed. The behavior was mimicked by intact R. We conclude that in addition to its negative regulatory role, the R subunit stimulates C activity via distal interactions.

The discovery of cAMP as a second messenger led eventually to the identification of PKA[1] with regulatory subunits that are the major receptors for cAMP [1]. PKA, ubiquitous in eukaryotic cells, regulates processes as diverse as growth, development, memory, metabolism, gene expression, and lipolysis [2]. The PKA holoenzyme exists as a complex of two C[1] subunits and an R[1] subunit dimer [1]. At low intracellular cAMP concentration, PKA is maintained as an inactive tetrameric holoenzyme complex (R_2C_2) consisting of a homodimer R_2 and two C. When intracellular concentration of cAMP is increased in response to specific stimuli, two cAMP molecules bind allosterically to each R and, as a consequence, the inhibition of C by R is released, allowing it to phosphorylate target proteins.

The C subunit is comprised of a small and a large lobe with the active site in a cleft between the two lobes. This fold, first described for PKA, defines the highly conserved protein kinase superfamily [3]. The small lobe provides the binding site for ATP, and the large lobe provides catalytic residues and a docking surface for peptide/protein substrates.

Mammalian Rs consist of the DDD[1] at the N terminus, through which two monomers of R dimerize, providing at a time a docking surface for A kinase anchoring proteins; at the C terminus two tandem cAMP-binding domains (CBD-A[1] and CBD-B[1]) and between a flexible linker region, which includes a basic substrate-like IS[1] that docks to the active site cleft of C in the absence of cAMP. This region has been subdivided into two to simplify the structural and functional studies: linker I, comprising the IS and the portion of the linker region N-terminal to it, and linker II containing the portion C-terminal to the inhibitor sequence [4]; (see Fig. 1).

Crystal structures of complexes between C and deletion mutants of RIα and RIIα have been recently solved [5–7]. The analysis of these structures reveals at least four distinct subsites on R that interact with C. One of the sites is the basic IS (RRXS or RRXA) that docks to the acidic active site cleft in C subunit. A second site is the charged and hydrophilic linker II, completely disordered in cAMP-bound R that becomes ordered at the interface with C subunit. The remaining two sites of interaction comprise both domains CBD-A and CBD-B.

We are interested in the study of the mechanism of activation of PKA and for this aim we have used three fungi as models, the dimorphic fungi *Mucor rouxii* and *Mucor circinelloides* and the yeast *Saccharomyces cerevisiae*. We have found that there is a great difference among species in the affinity between R and C. The interaction between R–C in PKA from *S. cerevisiae* has already been reported to be lower than the one shown by PKAs from mammals [8]. PKA from both *Mucor* models have an important difference when compared to

* Corresponding author. Fax: +54 11 45763342.
E-mail address: smoreno@qb.fcen.uba.ar (S. Moreno).

[1] *Abbreviations used:* PKA, cAMP dependent protein kinase; C, catalytic subunit; R, regulatory subunit; DDD, dimerization and docking domain; CBD-A, cAMP binding domain A; CBD-B, cAMP binding domain B; IS, inhibitory sequence; C_{Mr}, catalytic subunit from *Mucor rouxii*; C_{Mc}, catalytic subunit from *Mucor circinelloides*; C_{Sc}, catalytic subunit from *Saccharomyces cerevisiae*; R_{Mr}, regulatory subunit from *Mucor rouxii*; Pyk1, pyruvate kinase 1; C_b, catalytic subunit from *Bos taurus*.

0003-9861/$ - see front matter © 2008 Elsevier Inc. All rights reserved.
doi:10.1016/j.abb.2008.09.014

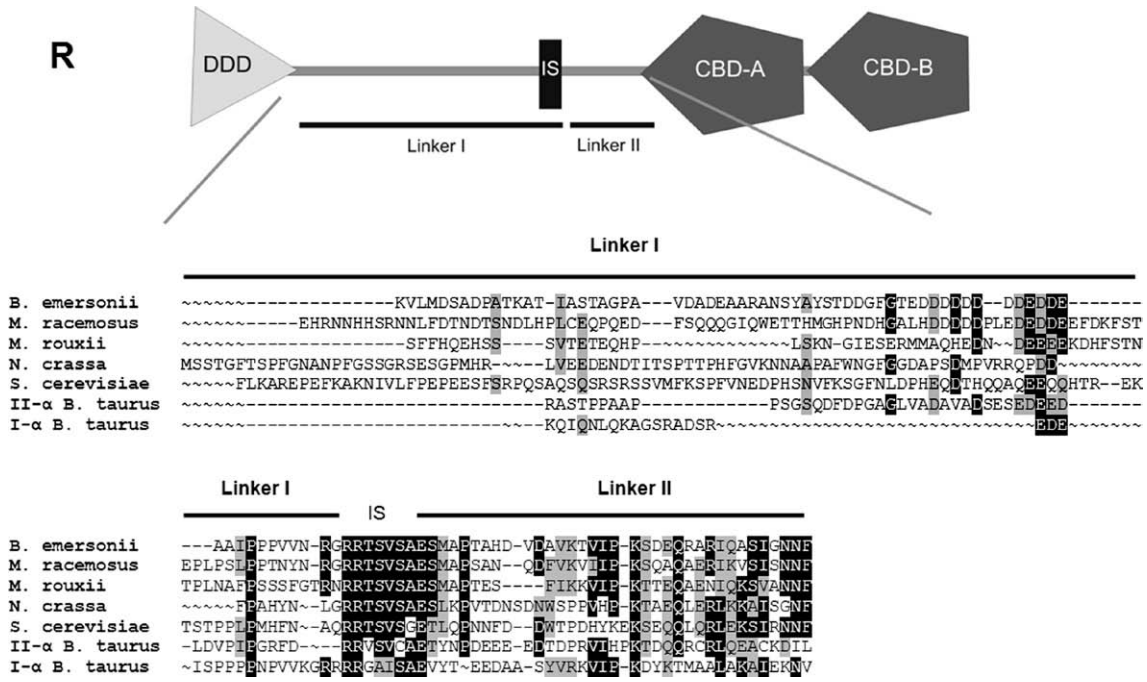

Fig. 1. Modular structure of R and multiple sequence alignment of the hinge region. The cartoon shows the general modular structure of R subunit. The alignment shows the hinge region of R subunits from *Bos taurus* (I-α and II-α), *Saccharomyces cerevisiae*, *Mucor rouxii*, *Mucor racemosus*, *Neurospora crassa* and *Blastocladiella emersonii*. Identical or similar residues are shaded according to the degree of identity or similarity.

mammalian PKA; from *in vitro* experiments we know they cannot be dissociated by the sole addition of cAMP even at low enzyme concentration and under non-equilibrium conditions; under these conditions cAMP bind only to the CBD-B sites [9]. However, the simultaneous addition of high salt (0.5 M NaCl) or polycations, together with cAMP, promotes the binding of cAMP to both CBD-A and CBD-B sites, and the dissociation of the subunits, suggesting additional ionic interactions in the holoenzymes [9–12].

Despite the high global degree of similarity among different R sequences from different species, there is striking sequence diversity in the hinge regions. The aim of this work is to investigate the importance of this region in the R–C interaction. The hypothesis is that the hinge region is a region of interaction, and that it could account in part for the different behavior of PKA holoenzymes among species. Particularly we now address, through a kinetic approach, the study of the linker region I using substrate and pseudosubstrate peptides derived from the IS domain containing part of the linker region I of the R subunits from *M. rouxii* and *S. cerevisiae*. The effect of these peptides is assayed on their own phosphorylation (substrate peptides) or on kemptide phosphorylation (pseudosubstrate peptides), and extended to a protein substrate. The effect of low concentrations of R from *Mucor* on the catalytic activity of C is also assayed. The results demonstrate that the linker region I participates in the interaction between R and C in both *Mucor* and *Saccharomyces* models, that there is some difference among species, and that the interaction with this region promotes an increase in the catalytic turnover of the C subunit, suggesting for the first time that R is not only an inhibitor of C activity in PKA but also a positive modulator of its catalytic efficiency.

Materials and methods

Materials

All chemicals were of reagent grade. Yeast growth medium supplies were from Difco Laboratories and Merck. Polyclonal anti-BCY (yN-19) and anti-goat IgG-peroxidase conjugated antibodies were from Santa Cruz Biotechnology Inc. Polyclonal antibody anti-*M. rouxii* R was prepared in rabbit [12]. Chemiluminescence Luminol Reagent was from GE Healthcare and [γ^{32}P]ATP was from Perkin-Elmer. Phospho-cellulose paper (P81) was from Whatman. Anti-rabbit IgG-peroxidase conjugated, ATP, cAMP, DEAE–cellulose, Phosphocellulose, Sephadex G-25 and horseradish peroxidase were from Sigma Chemical Co. Purified recombinant *Bos taurus* Cα was a generous gift from S. Taylor, University of California, San Diego. Nitrocellulose membrane was from MSI. EDTA-free protease inhibitor cocktail was from Roche Diagnostics GmbH. Peptides were chemically synthesized by GenScript Corporation.

Sequence analysis

cAMP-dependent protein kinase regulatory R from *B. taurus* I-α (gi 125192), *B. taurus* II-α (gi 125197), *S. cerevisiae* (gi 600015), *M. rouxii* (gi 285215), *M. circinelloides* (gi 119712284), *Neurospora crassa* (gi 6225583) and *Blastocladiella emersonii* (gi 285215) were collected from National Institute of Health GenBank. CBD-A, CBD-B and DDD were predicted by SMART (smart.embl-heidelberg.de) in all the analyzed sequences except for *N. crassa* which did not display a predictable DDD. The hinge region of each sequence was obtained from the difference between the full-length sequence and the predicted domains. Multiple sequence analysis of the hinge region was performed by ClustalW 1.8 using the default parameters. BioEdit 7.0.3 was used to edit sequence alignment.

Mucor rouxii PKA C purification

Fresh spores of *M. rouxii* (NRRL 1894) were grown to exponential phase in rich medium. The holoenzyme was prepared from mycelial powder through DEAE–cellulose and $(NH_4)_2SO_4$ precipitation. For most of the experiments C was isolated by dissociating sucrose gradient centrifugation with 0.5 M NaCl and 1 mM cAMP as described previously [13]. The fractions with maximum phosphotransferase

activity were pooled, freeze-dried and stored at −20 °C to use as enzyme source. The absence of R in these fractions was checked by Western blot, using polyclonal anti-*M. rouxii* R antibody. Before use, freeze-dried extracts were resuspended in the original volume of water and protease inhibitor cocktail. To perform the experiments of viscosity dependence of kinetic parameters, $C_{Mr}{}^1$ was obtained through cAMP–agarose affinity chromatography of the partially purified holoenzyme. Under these conditions, the holoenzyme is retained in the cAMP–agarose. The bound C was eluted with 0.5 M NaCl. The fractions with maximum phosphotransferase activity were pooled and used during the same day.

Mucor circinelloides PKA C purification

Mucor circinelloides strain R7B was grown to exponential phase in rich medium. $C_{Mc}{}^1$ was purified through DEAE–cellulose, $(NH_4)_2SO_4$ precipitation and cAMP agarose affinity chromatography as described above. The fractions with maximum phosphotransferase activity were pooled, freeze-dried and stored at −20 °C to use as enzyme source. The absence of R in these fractions was checked by Western blot, using polyclonal anti-*M. rouxii* R antibody. Before use, freeze-dried extracts were resuspended in the original volume of water and protease inhibitor cocktail.

Saccharomyces cerevisiae PKA C purification

The holoenzyme was prepared from 1115 wild-type (wt1115) yeast cells through $(NH_4)_2SO_4$ precipitation and C was isolated by dissociating sucrose gradient centrifugation with 0.5 M NaCl and 1 mM cAMP as in C_{Mr} preparation. Gradient profile and storage were performed as described above for C_{Mr} purification. The absence of R in the collected fractions was checked by Western blot, using polyclonal anti-BCY antibody. Before use, freeze-dried extracts were resuspended in the original volume of water and protease inhibitor cocktail.

Mucor circinelloides R expression and purification

$R_{Mc}{}^1$ was prepared by sucrose gradient centrifugation of crude extracts from *S. cerevisiae* strain S13-3A overexpressing R_{Mc} from pYES-R, a high copy number plasmid under the control of a galactose-dependent promoter. The strain S13-3A harbors a deletion mutation that abolishes Bcy1 endogenous expression [11]. The fractions with maximum cAMP binding activity were pooled, freeze-dried and stored at 20 °C until use. This R preparation is not cAMP-free.

Saccharomyces cerevisiae Pyk1[1] purification

The source of enzyme was the JT20454 strain, containing the plasmid pPyk101, which allows the overexpression of this protein under its own promoter. Pyk1 was prepared by two chromatography steps, DEAE–cellulose and phospho-cellulose, and $(NH_4)_2SO_4$ precipitation as previously described [14]. Pellets were stored at −20°C. The purification was monitored by Coomassie Blue staining of the different purification steps on SDS–PAGE. Before use, pellets were resuspended and desalted through Sephadex G-25. The quantification of purified Pyk1 was made by SDS–PAGE using BSA as standard.

PKA activity assays

Phosphotransferase activity of the *M. rouxii*, *S. cerevisiae* and mammalian Cα were assayed in a reaction mixture containing 50 mM Tris–HCl, pH 7.4, 0.1 mM [γ^{32}P]ATP (300 cpm/pmol when using peptidic substrates and 1500 cpm/pmol when using Pyk1 as substrate and for the experiments with R_{Mc}), 0.1 mM EGTA, 0.1 mM EDTA, 15 mM $MgCl_2$, 10 mM β-mercaptoethanol (Buffer A) and variable amounts of substrate peptides or Pyk1 in the absence or presence of non-phosphorylatable peptides, when indicated. When added, non-phosphorylatable peptides were preincubated with the enzyme in Buffer A at 4 °C for 10 min. When assaying the effect of R_{Mc} on kemptide phosphorylation by C_{Mc}, both subunits were preincubated at 30 °C for 30 min in buffer A (without addition of [γ^{32}P]ATP). In this case the reaction was started by addition of kemptide (final concentration 200 μM) and [γ^{32}P]ATP. The enzymatic assays were incubated at 30 °C for 15 min. Linear conditions were always used both for time and enzymatic protein concentration. In all the cases, except in Fig. 8, the amount of enzyme used in each reaction was 10 U (1 U corresponds to 1 pmol of phosphate incorporated per min to saturating concentrations of kemptide at 30 °C), which, in the case of pure bovine C subunit (C_b), corresponded to 0.15 pmol of enzyme. For Fig. 8 the following conditions were used: 2 U C_{Mc} and 0.02 pmol of pure C_b. Reactions using peptide substrates were processed by the phosphocellulose paper method [15]. The incorporation of phosphate into Pyk1 was determined by scintillation counting of phosphorylated protein excised from standard dried SDS–PAGE gels. Alternatively, SDS–PAGE dried gels were subjected to digital imaging analysis (Bio-Imaging Analyzer Bas-1800II and Image Gauge 3.12, FUJIFILM). In all the experiments kemptide phosphorylation was assayed as enzyme quality control and for comparative aims.

Viscosity dependence of kinetic parameters

The effect of viscosity on V_{max} and on V_{max}/K_m was assayed at 30 °C in the standard buffer A of PKA assays, with the addition of variable glycerol concentrations (0–40% v/v). The relative viscosities ($\eta\eta_0$) of reaction buffers containing glycerol were calculated relative to buffer A at 30 °C, using an Ostwald viscometer.

Data analysis

Data from peptide substrates were fitted to Michaelis–Menton curves using GraphPad Prism 4.02 version. K_m and *relative* k_{cat}, (*relative* k_{cat} = *peptide* V_{max}/*kemptide* V_{max}) were compared. Catalytic efficiency ($K_{sp}{}^*$) was calculated as the mean value of *relative* k_{cat}/mean value of K_m for each substrate peptide; relative specificity (relative k_{cat}/K_m), as the ratio of $K_{sp}{}^*$ of different peptides from the same source (47-S/8-S; 18-S/8-S; 47-S/18-S). In the viscosity experiments k_{cat} *ratio* and k_{cat}/K_m *ratio* are the ratios of the V_{max} and V_{max}/K_m obtained in the absence of viscogen to the one in its presence. V_{max}/K_m values were calculated from the slope of the Lineweaver–Burk linear plots. Data from these assays (k_{cat} *ratio* or k_{cat}/K_m ratio vs relative viscosity) were fitted to linear function. The slopes were estimated and compared.

Statistical treatment of results

Each experiment was performed three times, in which each data point was assayed in duplicate. To evaluate the effect of 10Nt-M on kemptide phosphorylation by C_{Mr}, the effect of 18-A-S on Pyk1 phosphorylation by C_{Sc} and the effect of R_{Mc} on kemptide phosphorylation of C_{Mc} and $C_b{}^1$ a one-way ANOVA was applied. In all cases Tukey post hoc comparisons were performed.

Results

Sequence analysis

In order to find possible sites of interaction in the hinge region of R that could account for the differences in affinity between R

and C observed among species we took a closer look to this region by performing sequence alignment of some fungal R, together with bovine RIα and RIIα as a reference (Fig. 1). The R sequences included correspond to biochemically characterized PKAs. From the alignment it can be observed that the most conserved part of the hinge region corresponds to the IS (RRXS). There is also some degree of conservation toward the C terminus of the IS, in the linker II region. The linker I region is very diverse and therefore suitable as a candidate region for the observed interspecific difference in affinity with C subunit.

There are already some results from Surface Plasmon Resonance and kinetic analyses of mammalian mutant C that suggest that the sequence immediately N terminal to the IS in RI and RII interacts with different sites at the proximal region of the active site cleft in C [16]. Besides, the region N terminal to the pseudosubstrate site of the protein kinase inhibitor (PKI) is also important for the interaction with C as it forms an amphipathic α-helix that binds to a hydrophobic pocket on the surface of the large lobe of C [17]. Kinetic experiments performed with deletion mutants of R from the PKA from *M. circinelloides* demonstrate that the cluster of acidic residues (−19 to −34 of the IS) in linker I of R_{Mc} participate in the interaction with C_{Mc} [11].

Peptide kinetic analysis: substrate peptide approach

Based on the sequence analysis and the results from the literature [11,16,17], we addressed the question of the role of the proximal linker I region on R–C interaction through a kinetic approach, in which we studied the effect of several peptides on the phosphorylating activity of *M. rouxii* (C_{Mr}), *S. cerevisiae* (C_{Sc}) and bovine (C_b) catalytic subunits. The peptide sequences correspond to the IS plus a variable region toward the N terminus of R_{Mr} and R_{Sc}, between residues P−42 and P+4 (relative to the phosphorylatable Ser at P 0) (Table 1). We chose this region because it is different among species, mainly in the nature of the amino acids. In some species like *Mucor* sp. it includes a cluster of acidic residues. Some of the synthetic peptides are phosphorylatable substrates as they have a Ser in the IS; while in others, the Ser has been replaced by Ala. Our rationale was to compare the affinity of the non-phosphorylatable peptide-C complexes by estimating the inhibition constant (K_i) for kemptide phosphorylation. This parameter is a good measure of affinity since it reflects substrate binding. But, to our surprise, the peptides did not behave as competitive inhibitors. Instead, they had a dual effect: they inhibited at high concentrations, but they increased the catalytic activity when the non-phosphorylatable peptide/kemptide ratio was low (see below and Fig. 5). As an approximation, we therefore turned to substrate peptides and estimated the steady-state kinetic parameters, although we are aware they do not provide a direct measure of the affinity of the substrate for the kinase (K_d). We estimated the K_m and V_{max} relative to kemptide V_{max} (from now on *relative* k_{cat}) for the phosphorylation of six substrate peptides by the three C: C_{Mr}, C_{Sc} and C_b (Fig. 2). We expressed the results as relative k_{cat} instead of k_{cat} in order to compare this parameter between experiments, since we could not estimate enzyme concentration so as to give an absolute value.

Table 1
Synthetic peptides derived from R_{Mr} and R_{Sc}. Nomenclature: the number is the length of the peptide. Second letter stands for Serine or Alanine in the phosphorylation site and third letter stands for the organism.

Name	Sequence	Organism
8-S-M	RRTSVSAE	*M. rouxii*
8-S-S	RRTSVSGE	*S. cerevisiae*
18-S-M	FPSSSFGTRNRRTSVSAE	*M. rouxii*
18-S-S	PPLPMHFNAQRRTSVSGE	*S. cerevisiae*
18-A-M	FPSSSFGTRNRRTAVSAE	*M. rouxii*
18-A-S	PPLPMHFNAQRRTAVSGE	*S. cerevisiae*
47-S-M	ESERMMAQHEDNDEEEEKDHFSTNTPLNA FPSSSFGTRNRRTSVSAE	*M. rouxii*
47-S-S	SGFNLDPHEQDTHQQAQEEQQHTREKTSTP PLPMHFNAQRRTSVSGE	*S. cerevisiae*
10Nt-M	FPSSSFGTRN	*M. rouxii*
NRP1	IRTGRTLNDR	
NRP2	LKKGDTYVSI	
Kemptide	LRRASLG	*S. scrofa*

A first observation derived from the analysis of the data from Fig. 2 is that the K_m values of the two fungal enzymes for the lower sized peptides (kemptide and 8-S) are higher than the one for C_b; however for the longer peptides (18-S and 47-S) all the enzymes seem to have the same apparent affinity. It has already been reported that the apparent affinities of C_{Mr} and C_{Sc} toward short peptides are lower than for C_b [13,14,18]. The differences observed for the short peptides, such as 8-S-M or 8-S-S, do not reflect the behavior of the hinge R–C interaction as it is not maintained for longer peptides. A similar behavior has been observed for pyruvate kinase 1 (Pyk1), a PKA substrate in *S. cerevisiae*; its K_m does not differ between C_{Sc} and C_b, despite the difference observed between these enzymes in the K_m for a peptide that corresponds to the phosphorylation site of Pyk1 as well as for kemptide [14].

A second observation derived from Fig. 2 is that the three C display the following general behavior: the longer the peptides, the higher their *relative* k_{cat} and the lower their K_m. The consequence of this change is a general increase in substrate specificity for each C with the length of the substrate, as judged by the catalytic efficiency (K_{sp}^*) estimated as the ratio of the mean-values of *relative* k_{cat} and K_m derived from Fig. 2 and shown in Table 2. However the degree of change in these parameters for each enzyme is different. Fig. 3 shows the relative (k_{cat}/K_m) of each enzyme comparing the data of the longer peptides 18-S and 47-S (the *M. rouxii* series or the *S. cerevisiae* series) with their respective 8-S parental peptide. It can be observed that the increase in efficiency attained by C_{Mr} and $C_{Sc,}$ reflected by the ratio 47-S-M/8-S-M, is around 60- and 30-fold, respectively; however the change in efficiency for C_b is not greater than 10-fold. The participation of the region N terminal to the IS of the linker I domain of R in these two fungal systems seems to be different from the mammalian holoenzyme. For both fungal C the gain of catalytic efficiency that corresponds to the region immediately N terminal to the IS (P-4 to P-13) is bigger than the one that corresponds to the region beyond (P-14 to P-42): the ratio of efficiencies 18-S/8-S is between 6.6 and 18.5, while the ratio 47-S/18-S is between 1.7 and 3.7. Both C_{Mr} and C_{Sc} have a preference for 18-S-M over 18-S-S (18-S-M relative specificity is higher than 18-S-S). This suggests that the region from P-4 to P-13 could account at least in part for the differences observed in R–C affinity among species. Since an Arg at P-6 of PKI is important for binding C [17,19] it is possible that the Arg at P-5 of R_{Mr} could be responsible for the higher specificity observed toward 18-S-M, displayed by both fungal enzymes, when compared to 18-S-S. Although in a rather small degree, the region beyond (from P-14 to P-42) seems to have a species-specific selectivity since the ratios 47-S/18-S are higher when assaying one C with the peptide pairs derived from its corresponding homologous R (Fig. 3, right bars). This would imply that this region of R, as well as an interacting complementary C surface might be contributing to the difference in R–C interaction. In the case of R_{Mc} we have already demonstrated that a deletion of the cluster of acidic residues in the region P-14 to P-42 decreases the interaction of R_{Mc} with C_{Mc}, but not the interaction with C_b [11].

The results of the change in kinetic parameters with the length of the peptide described above, suggest that in both *M. rouxii* and *S. cerevisiae* holoenzymes the two regions N terminal to IS, namely P-4 to P-13 and P-14 to P-42 contribute to the R–C interaction,

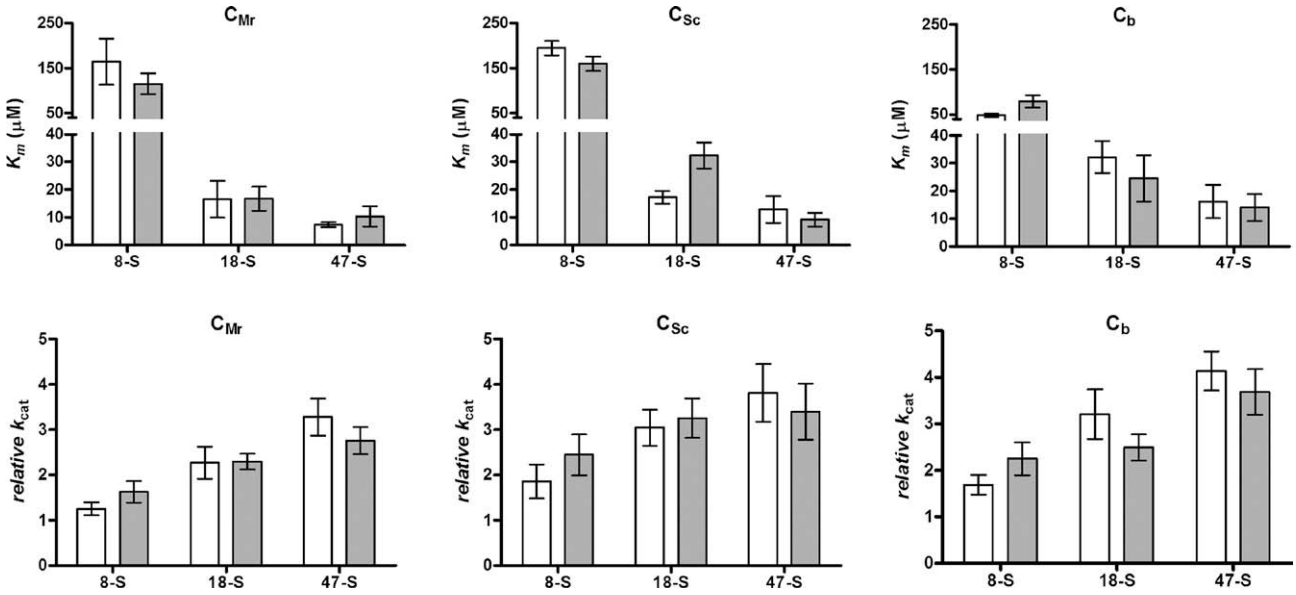

Fig. 2. Steady-state kinetic parameters. Aliquots of partially purified preparations of C_{Mr}, C_{Sc} and C_b were used to determine K_m and V_{max} values for the substrate peptides of Table 1. White bars represent peptides derived from *M. rouxii* R sequence, and gray bars represent peptides derived from *S. cerevisiae* R sequence. Relative k_{cat} is defined as the ratio between peptide/kemptide V_{max}. Values are means ± SEM ($n = 3$).

Table 2
K_{sp}^* of substrate peptides for C_{Mr}, C_{Sc} and C_b. Catalytic efficiency (K_{sp}^*) was calculated as the mean value of *relative* k_{cat}/mean value of K_m (mM) for each substrate peptide from the data of Fig. 2.

Peptide	K_{sp}^*		
	C_{Mr}	C_{Sc}	C_b
8-S-M	0.008	0.010	0.035
8-S-S	0.014	0.015	0.028
18-S-M	0.138	0.176	0.099
18-S-S	0.137	0.101	0.101
47-S-M	0.444	0.297	0.254
47-S-S	0.266	0.370	0.261

being the contribution of the proximal regions much more important than the distal ones.

Effect of solvent viscosity on kinetic parameters

The behavior of the steady-state kinetic parameters *relative* k_{cat} and K_m, observed with C_{Mr} and C_{Sc} is in accordance with the clamp model proposed by Lieser et al. for protein kinases [20]. This model explains the decrease of K_m and the increase of k_{cat} of a protein substrate, compared with the peptide derived from the consensus sequence, through a direct thermodynamic coupling of the substrate binding and chemical transfer steps. A fast and highly favorable phosphoryl transfer step can enhance interactions with a consequent increase in apparent affinity. The kinetic pathway for substrate phosphorylation by a protein kinase is composed of three fundamental events: substrate binding, the phosphoryl transfer step and the irreversible, net product release. While the dependence of substrate concentration on the reaction rate provides an estimate of the steady-state parameters k_{cat} (turnover number) and K_m, the relationship between these parameters and each of the reaction steps can be difficult to resolve [20].

In order to determine which of the three steps, phosphate transfer, substrate binding or product release, were rate limiting for substrate phosphorylation we applied the viscosity method. This method is based in the fact that bimolecular events (substrate binding and product release) are expected to be influenced by solvent viscosity whereas the unimolecular steps (phosphoryl transfer step) are not. Either k_{cat} or k_{cat}/K_m as a ratio in the absence and presence of added viscosogens relates linearly with the relative

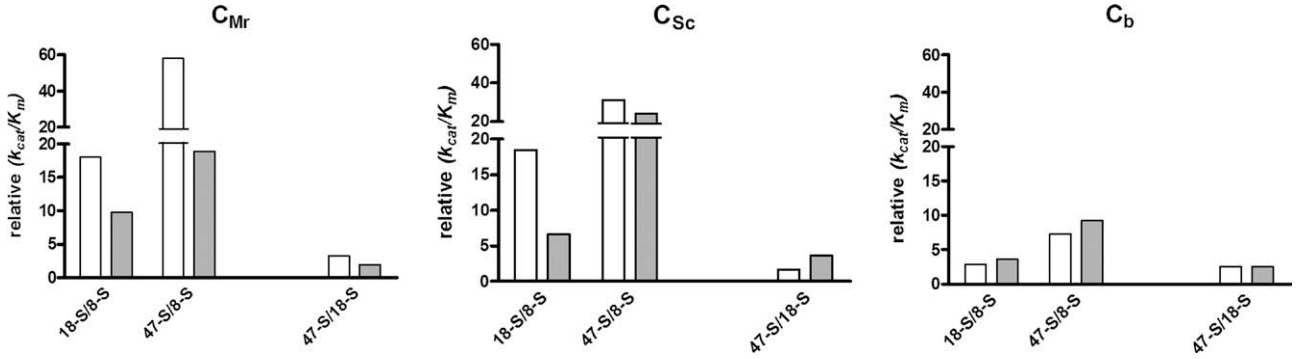

Fig. 3. Relative specificities of the catalytic subunits for the different substrate peptides. Relative specificity (relative (k_{cat}/K_m)), defined as the ratio of k_{cat}/K_m of different peptides of the same source, was calculated from the data of Table 2 for the three C. The group of bars at the left end represent the ratio between the k_{cat}/K_m of 18-S and 47-S peptides referred to 8-S; while those at the right end represent the ratio of the k_{cat}/K_m between 47-S and 18-S. White bars represent peptides derived from *M. rouxii* R sequence, while gray bars represent peptides derived from *S. cerevisiae* R sequence.

solvent viscosity. The slopes give information on the catalytic step (k_3) as compared to the product release step (k_4) (k_{cat} plot) or to the substrate dissociation step (k_{-2}) (k_{cat}/K_m plot) [21].

Fig. 4B shows the effect of viscosity on the k_{cat} of C_{Mr} for four peptide substrates: kemptide, 8-S-M, 18-S-M and 47-S-M. The effect of viscosity on k_{cat} was performed in parallel using the same substrates and C_b as a reference (Fig. 4A). The slope values for this plot fall between the theoretical limits of 0 and 1. These limits correspond, respectively, to reactions in which either the phosphoryl transfer step or the net product release, are rate limiting. When using kemptide or 8-S-M as substrates, the effect of the viscosity on k_{cat} is intermediate (slopes = 0.5 and 0.6, respectively), while when using 18-S-M or 47-S-M the effect of viscosity is maximum (slope = 1). Intermediate values imply that phosphoryl transfer and net product release are partially rate determining. For C_b we observed (Fig. 4A) that when using as substrates the three peptides derived from R_{Mr}, the k_{cat} was fully affected by viscosity (slope = 1 for all the substrates). The high viscosity effect of C_b, with a small peptide substrate such as kemptide, has already been described and suggested to be due to the extremely high phosphotransfer rate of this enzyme [20]. Fig. 4C shows the influence of viscosity on the k_{cat}/K_m ratio. The theoretical limits of this slope also fall between 0 and 1. The limit of 1 is approached when the substrate is sticky ($k_3 >> k_{-2}$). The results show slopes of 0, 0.1 and 0.2 for 8-S, 18-S and 47-S, respectively, indicating that even though substrates 18-S and 47-S are longer than 8-S, with new contact points with C subunit, they are not transformed into sticky substrates. The results suggest that for C_{Mr}, both the phosphate transfer and the product release steps contribute to the enzyme turnover when the substrate is a short peptide. However, when using the peptides that include part of the linker region of R, the phosphate transfer is faster, without an increase in substrate stickiness, being now the product release the rate limiting step. Therefore contacts outside the active cleft might have an impact on the phosphate transfer rate for this enzyme, in accordance with the clamp model proposal.

Peptide kinetic analysis: dual effect of non-phosphorylatable peptides

As stated above, our original rationale to study the role of the proximal linker I region on R–C interaction was to assay the effect of the non-phosphorylatable peptides 18-A-M and 18-A-S on the kemptide phosphorylating activity of C. Our expectation was to find a competitive inhibition; instead we observed a dual behavior: activation at a low ratio pseudosubstrate:substrate concentration and inhibition at a high ratio. The same behavior was displayed by the three C for both 18-A-M and 18-A-S. Representative experiments of these results are shown in Fig. 5. The effect of two non-related peptides (NRP1 and NRP2, see Table 1) was assayed to discard non-specific effects. None of these two peptides had an effect on either C_{Mr} or C_{Sc} activities (insets of Fig. 5). The phosphorylation of 18-A-M and 18-A-S by C subunit was also ruled out (data not

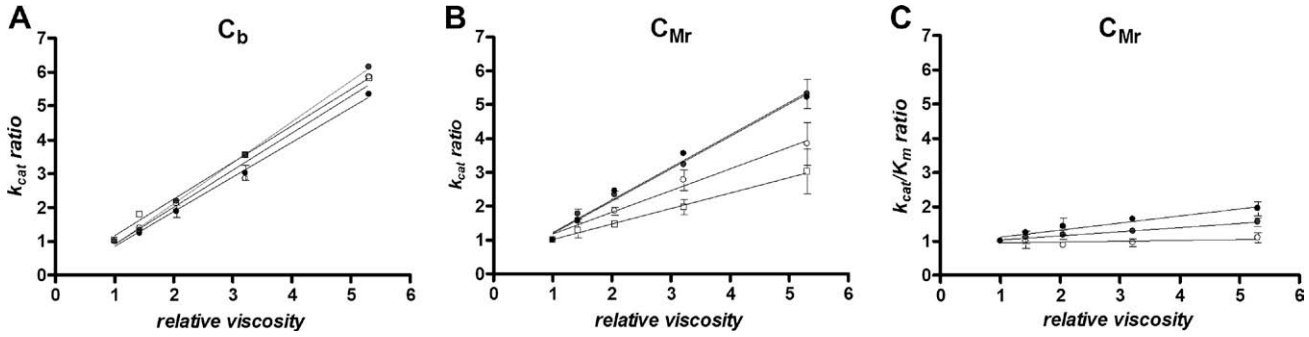

Fig. 4. Effect of solvent viscosity on kinetic parameters. The V_{max} of C_b (A) and C_{Mr} (B) and the V_{max}/K_m of C_{Mr} (C) using as substrates: kemptide (white square) 8-S-M (white circle), 18-S-M (gray circle) and 47-S-M (black circle) were estimated in the absence and in the presence of different amounts of glycerol. The k_{cat} *ratio* and k_{cat}/K_m *ratio* defined as the ratio of the V_{max} and V_{max}/K_m obtained in the absence of viscogen to the one in its presence, respectively, was plotted against the relative viscosity. Solid lines correspond to the best-fitting linear equation. Error bars correspond to duplicates. The graphics show representative experiments.

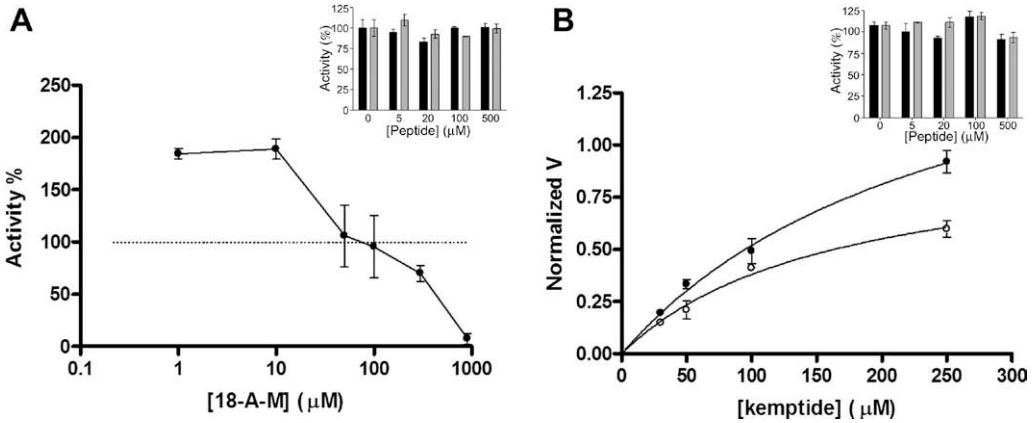

Fig. 5. Effect of 18-A peptides on kemptide phosphorylation. (A) Effect of 18-A-M on kemptide (100 μM) phosphorylation by C_{Mr}; the activity in the absence of 18-A-M is taken as 100%. (B) Effect of 18-A-S on kemptide phosphorylation by C_{Sc}, in the absence (open symbols) and presence (filled symbols) of 6 μM 18-A-S. Solid line represents the best-fitting curve according to Michaelis–Menton equation. *V* values in the *y*-axis are normalized relative to V_{max} in the absence of 18-A-S. Insets: effect of two non-related peptides, NRP1 (black bars) and NRP2 (gray bars) on kemptide (saturating concentration) phosphorylation by C_{Mr} (A) and C_{Sc} (B). The graphics show representative experiments and error bars correspond to duplicates.

shown), especially for 18-A-M that has three Ser in a row. It is difficult to ascertain the real degree of activation, since the observed results (Fig. 5A) is a consequence of the dual activation–inhibition role of the assayed 18-A-M and 18-A-S. At low 18-A and high kemptide concentrations the activating effect is evidenced, while at high 18-A concentration, the inhibitory effect predominates. From the results of Fig. 5B, it can be concluded that the addition of 18-A does not produce an important change in kemptide K_m, if any.

A pseudosubstrate consensus sequence is expected to have a competitive behavior toward the substrate; we thought that the N-terminal region of 18-A-M or 18-A-S peptides might be responsible for the activating effect. We therefore evaluated the effect of a peptide that corresponds only to this 10 residue-region of RMr (10Nt-M) (Table 1) on the phosphorylation of kemptide by C_{Mr} (Fig. 6). A significant activation of 2.5–3-fold was observed at kemptide concentrations below, within and above the K_m (34 μM), suggesting that the interaction of this region in the R subunit with the C subunit promotes an increase in the activity. The fact that the degree of activation did not change with kemptide concentration suggests that the effect is mainly on the catalytic activity and not in the K_m. The same results were obtained when the addition of 18-A-S was assayed on the phosphorylation of kemptide by C_{Sc} (Fig. 5B). This result suggests that the interaction of this region in the R subunit with the C subunit promotes an increase in the catalytic activity.

To determine whether 18-A peptides could be able to activate not only the phosphorylation of peptides but also of protein substrates, we assessed the effect of 18-A-S on *S. cerevisiae* pyruvate kinase 1 (Pyk1) phosphorylation by its corresponding C_{Sc}. Pyk1 has been shown to be a substrate of PKA in *S. cerevisiae* [22]. Activity of C_{Sc} toward a saturating concentration of Pyk1 (40 μM) was assayed in the absence or in the presence of 18-A-S (0–400 μM). Fig. 7 shows that in the 3–75 μM range, 18-A-S promoted a significant activation on the phosphorylation of Pyk1 by C_{Sc}. This 2-fold level of stimulation is similar to the one observed for peptides, shown in Fig. 5. Higher concentrations of the pseudosubstrate 18-A-S produced the expected inhibition of the kinase activity.

Dual effect of R on kemptide phosphorylation

In the above-mentioned experiments we observed that the pseudosubstrate peptides 18-A-S and 18-A-M, had a stimulating effect in trans, on the phosphorylating activity of either C_{Mr} or C_{Sc} toward a peptide or even toward a whole protein. These two peptides correspond to sequences of the respective R. We therefore wondered whether the full-length R could have the same dual effect of the non-phosphorylatable peptides. The classical inhibitory effect of R on C activity has been already demonstrated [21,11,23].

In order to evaluate whether R could display a dual effect on C activity we assayed the effect of small concentrations of R_{Mc} (<0.1 nM) on the catalytic activity of both C_{Mc} and C_b using kemptide as substrate. We chose these concentrations, since we had

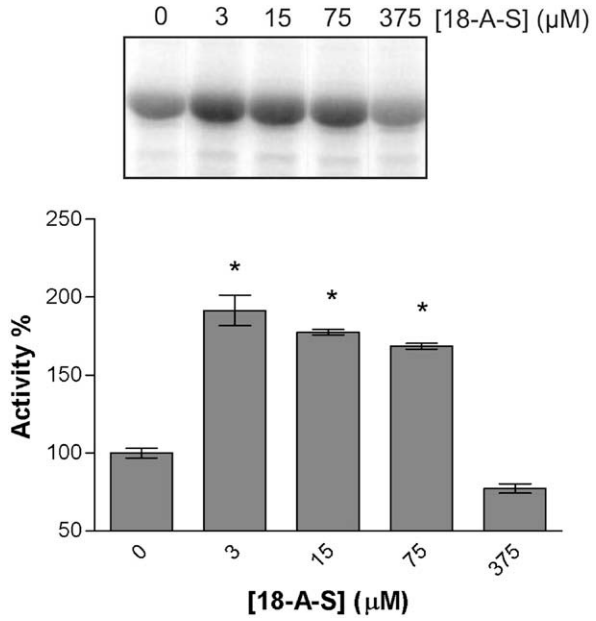

Fig. 7. Effect of 18-A-S on Pyk1 phosphorylation by C_{Sc}. Activity of C_{Sc} at saturating concentrations (40 μM) of Pyk1 was assayed in the absence and in the presence of different concentrations of 18-A-S (0–400 μM). The activity was estimated from a radioactive SDS–PAGE (inset) as described in Materials and methods. The graphic shows a representative experiment. Error bars correspond to duplicates. Asterisks indicate significant differences ($p < 0.01$) compared with the first column (without 18-A-S).

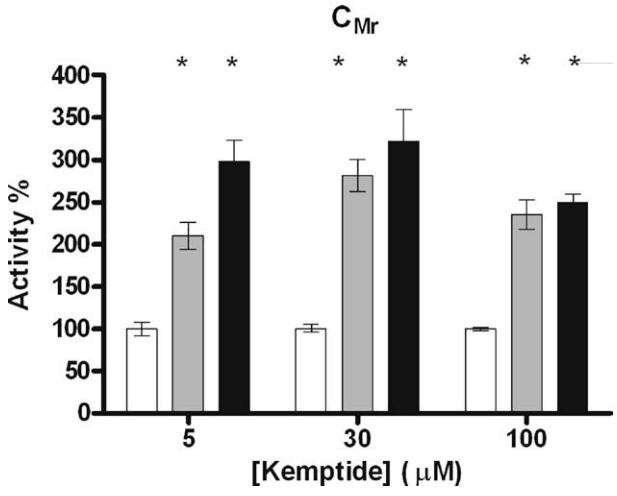

Fig. 6. Effect of 10Nt-M on kemptide phosphorylation by C_{Mr}. Activity of C_{Mr} at 5, 30 and 100 μM of kemptide was assayed in the absence (white bars) and in the presence of 25 μM (gray bars) and 100 μM (black bars) of 10Nt-M. The graphics show representative experiments and error bars correspond to duplicates. Asterisks indicate significant differences ($p < 0.01$) compared with the white bars (without 10Nt-M).

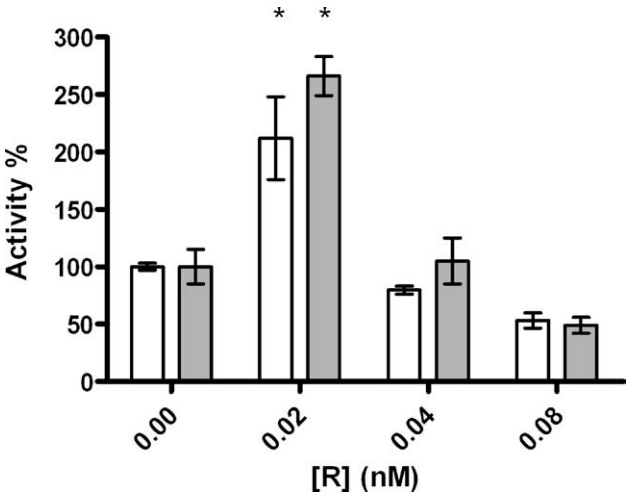

Fig. 8. Effect of R_{Mc} on kemptide phosphorylation by C_b and C_{Mc} Activity of C_{Mc} (gray bars) and C_b (white bars) at saturating concentrations (300 μM) of kemptide was assayed in the absence and in the presence of R_{Mc} (0–0.08 nM). The graphic shows a representative experiment. Error bars correspond to duplicates. Asterisks indicate significant differences ($p < 0.01$) compared with the first columns (without R_{Mc}).

already observed [11] that, under the experimental setting used, concentrations >0.1 nM of fungal R produced a clear inhibition of catalytic activity of both C_{Mc} and C_b. Fig. 8 shows that at around 0.02 nM R there is a significant activation of 2.5-fold of the catalytic activity of C toward kemptide. At concentrations higher than 0.1 nM of R, a clear inhibitory effect is observed [data not shown; 11]. This is the first time that a dual, activating–inhibitory effect of R on C activity is described. This result resembles the results described in Fig. 5 for both non-phosphorylatable peptides, 18-A-S and 18-A-M.

Discussion

In this work we have analyzed the kinetic behavior of three C subunits, C_{Mr}, C_{Sc} and $C_{b,}$ toward phosphorylatable peptides derived from the linker I region of R_{Mr} and $R_{Sc.}$. The results indicate that the longer the peptides the higher the *relative* k_{cat} and the lower the K_m. Although this effect was qualitatively the same with the three C, it was quantitatively much greater with the two fungal C. The change in steady-state parameters for both fungal C suggests that in both holoenzymes the region from P-4 to P-42 of R contributes to the R–C interaction. The region from −13 to −42 of R could account, at least in part, for the differences observed in R–C affinity among species, since the increase in specificity constant of C_{Mr} and C_{Sc} when comparing 18-S with 47-S peptides is bigger when using C with their corresponding phosphorylatable peptides (Fig. 3, right set of bars).

The great increase in apparent affinity of the phosphorylatable peptides 18-S and 47-S when compared to the 8-S, for both fungal systems, seems to fit within the clamp model, as judged by the change in steady-state kinetic and the dependence of V_{max} on viscosity with the length of the peptides. According to this model, there could be a direct thermodynamic coupling between the binding of 18-S and 47-S peptides and the chemical transfer step. This coupling leads to an increase in the phosphoryl transfer rate with a consequent increase in the apparent affinity. In Fig. 9 we illustrate the clamp model as a cis-activation mechanism, in comparison to the basal activity, in which the region of the peptides N-terminal to the IS generate, probably through a conformational change in the C subunit, an increase in the phosphate transfer rate. The fact that the apparent affinity of 8-S and kemptide for C_{Mr} and C_{Sc} is lower than for C_b, together with the difference in the response to viscosity, might reflect that the catalytic turnover of C_{Mr} and C_{Sc} is lower than the one of C_b. It is probable that the activation effect of the linker region-peptides ("clamp" effect) on C_b kinetics is masked by the exceptionally high catalytic turnover of this enzyme [20].

The non-phosphorylatable versions of the linker region peptides, 18-A-S or 18-A-M, when bound to their corresponding C subunits, inhibit their activity, as expected. However this inhibition is not competitive. When the kemptide concentration is high, the inhibitory effect is minimized and an increase of basal activity could be observed. Making a comparison of what happens with the 18-S linker peptides, we named this effect as a trans activation in

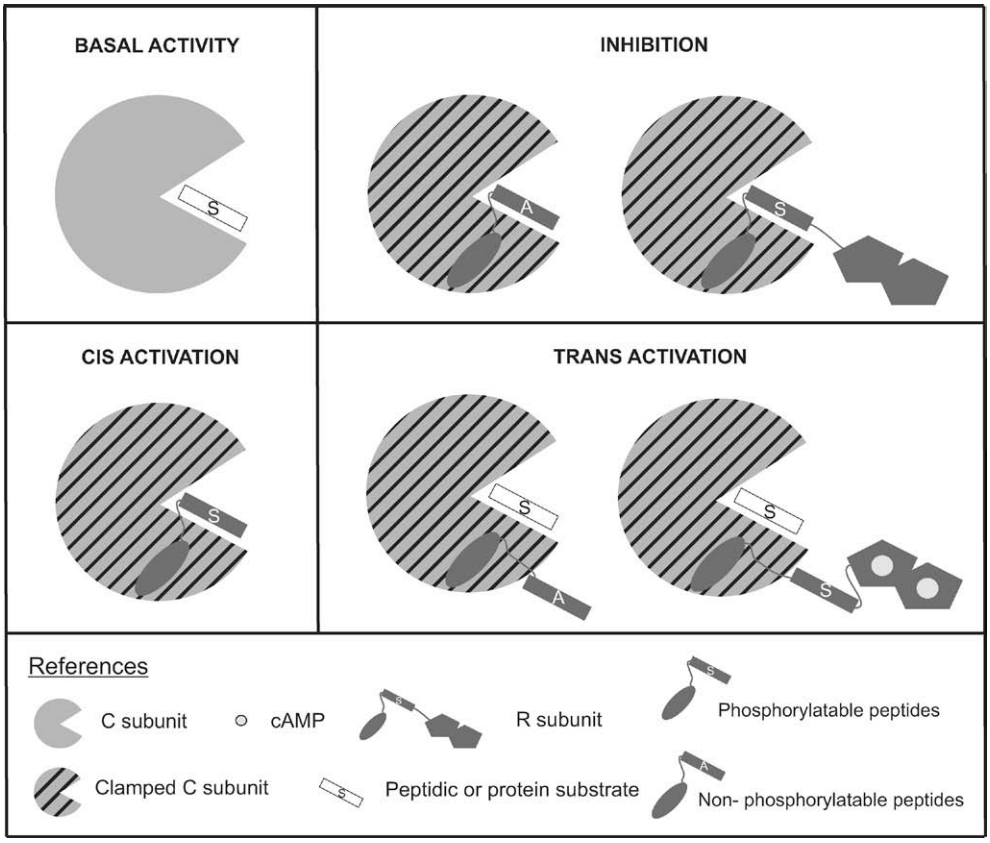

Fig. 9. Model for the dual effect of peptides and R on C phosphotransferase activity. Basal activity of C subunit is represented as a plain scheme of C phosphorylating a peptidic or protein substrate. The increase in apparent affinity and in phosphotransferase activity of 18-S or 47-S linker peptides is represented as a cis-activation effect produced by a clamp-docking site of the peptide on C besides the phosphorylation site. Clamped C in the model is represented by a striped scheme. Inhibition in this model is represented by the interaction of the inhibitory peptides 18-A to C, or of R subunit to C. Notice than under these conditions, C subunit is already clamped (striped), although activity cannot be measured. The clamp effect of non-phosphorylatable linker peptides 18-A on the phosphorylation of peptidic or protein substrates is represented as the result of a trans-activation effect derived from the clamp/allosteric interaction of the non-phosphorylatable peptide on C. The clamp effect of R on C phosphorylation of a substrate is shown as a trans-activation effect produced by a clamp docking domain of a region N-terminal to the IS of R that allosterically increases the phosphotransfer rate of the C subunit, once the interaction between C and R is loosened by the binding of cAMP.

which we figure out that the 18-A peptide is bound to the C subunit through a docking interaction, simultaneously with kemptide or protein substrate, exerting a clamp effect in trans (Fig. 9). A support for this model is obtained through the use of the 10Nt-M, in which we could dissociate the allosteric-docking effect from the inhibitory effect (Fig. 6). It is worth noticing that in the model of inhibition in Fig. 9, with the 18-A peptide bound, the C subunit is already drawn as clamped, although activity cannot be measured under this condition.

We show in this work for the first time a dual behavior of R on C: a novel activating effect and a classic inhibitory effect (Fig. 9 inhibition), illustrated with R of *M. circinelloides* when added to its homologous C_{Mc}, as well as to mammalian C_b. A feasible interpretation, illustrated in Fig. 9 (trans activation) is the following. When there are low levels of cAMP in the cell, the inhibitory effect predominates. However when part of the interactions that maintain the high affinity binding between R and C in the holoenzyme are weakened, it is possible that the region N-terminal to the IS of R still remains bound to the C subunit. This interaction, as if it were a docking site, improves the phosphoryl transfer rate of substrates in trans. Docking interactions in protein kinase and phosphatase networks are well known, not only to increase enzyme–substrate specificity, but also to govern the binding of kinases and phosphatases to each other and other effectors [24]. Overall, the primary role of docking interactions appears to be tethering. However there are some examples in which docking interactions play an important role in altering protein conformation and allosterically regulating activity [24]. The regulation of C activity by R, described in this work, fits into the model of docking and allosteric regulation. A modern view of substrate phosphorylation by PKA *in vivo* is that holoenzyme and substrate are linked and localized through interaction via anchoring proteins. We propose that within this context, and in the presence of cAMP, R can remain in contact with C through at least the linker region amino terminal to the IS, and that this docking allosterically improves the phosphorylation of a substrate in trans.

Acknowledgments

This work was supported by grants from University of Buenos Aires (X-270), Consejo Nacional de Investigación Cientifica y Tecnológica (CONICET) (PIP 5239), and Agencia Nacional de Promoción Científica y Tecnológica (PICT 01-08793 and PICT 05-38212). J.R. and J.O. are doctoral fellows from CONICET. We thank Paula Portela for helpful discussion and insightful critics.

References

[1] S.S. Taylor, C. Kim, D. Vigil, N.M. Haste, J. Yang, J. Wu, G.S. Anand, Biochim. Biophys. Acta 1754 (2005) 25–37.
[2] K. Taskén, E.M. Aandahl, Physiol. Rev. 84 (2004) 137–167.
[3] S.S. Taylor, D.R. Knighton, J.H. Zheng, J.M. Sowadski, C.S. Gibbs, M.J. Zoller, Trends Biochem. Sci. 18 (1992) 84–89.
[4] D. Vigil, D.K. Blumenthal, S.S. Taylor, J. Trewhella, J. Mol. Biol. 357 (2006) 880–889.
[5] C. Kim, N.H. Xoung, S.S. Taylor, Science 307 (2005) 690–696.
[6] C. Kim, C.Y. Cheng, S.A. Saklanha, S.S. Taylor, Cell 130 (2007) 1032–1043.
[7] J. Wu, S. Brown, S. von Daake, S.S. Taylor, Science 318 (2007) 274–279.
[8] J. Kuret, K.E. Johnson, C. Nicolette, M.J. Zoller, J. Biol. Chem. 263 (1988) 9149–9154.
[9] C. Paveto, S. Passeron, J.D. Corbin, S. Moreno, Eur. J. Biochem. 179 (1989) 429–434.
[10] S. Moreno, R. Pastori, S. Passeron, Cell. Biochem. 52 (1983) 13–16.
[11] J. Ocampo, S. Moreno, S. Rossi, Biochem. Biophys. Res. Commun. 362 (2007) 721–726.
[12] S. Rossi, M. Guthmann, S. Moreno, Cell. Signal. 4 (1992) 443–451.
[13] V. Zaremberg, A. Donella-Deana, S. Moreno, Arch. Biochem. Biophys. 381 (2000) 74–82.
[14] P. Portela, S. Moreno, S. Rossi, Biochem. J. 396 (2006) 117–126.
[15] R. Roskoski, Methods Enzymol. 99 (1983) 3–6.
[16] X. Cheng, C. Phelps, S.S. Taylor, J. Biol. Chem. 276 (2001) 4102–4108.
[17] D.R. Knighton, J.H. Zheng, L.F. Ten Eyck, N.H. Xuong, S.S. Taylor, J.M. Sowadski, Science 253 (1991) 414–420.
[18] C.L. Denis, B.E. Kemp, M.J. Zoller, J. Biol. Chem. 266 (1991) 17932–17935.
[19] J. Reed, J.S. De Ropp, J. Trewhella, D.B. Glass, W.K. Liddle, E.M. Bradbury, V. Kinzel, D.A. Walsh, Biochem. J. 264 (1989) 371–380.
[20] S.A. Lieser, B.E. Aubol, L. Wong, P.A. Jennings, J.A. Adams, Biochim. Biophys. Acta 1754 (2005) 191–199.
[21] L. Wong, P.A. Jennings, J.A. Adams, Acc. Chem. Res. 37 (2004) 304–311.
[22] P. Portela, S. Howell, S. Moreno, S. Rossi, J. Biol. Chem. 277 (2002) 30477–30487.
[23] M.J. Zoller, J. Kuret, S. Cameron, L. Levin, K.E. Johnson, J. Biol. Chem. 263 (1988) 9142–9148.
[24] A. Reményi, M.C. Good, W.A. Lim, Curr. Opin. Struct. Biol. 16 (2006) 676–685.